Electromagnetic Characterization of Chiral Media

J. Margineda, G. J. Molina-Cuberos, NúñezM. J.,
A. J. García-Collado and E. Martín

Additional information is available at the end of the chapter

http://dx.doi.org/10.5772/51539

1. Introduction

The electromagnetic characterization of materials is a fundamental problem in many research areas of Electromagnetism. The goal is to determine the electrical permittivity and magnetic permeability, which make up the usual constitutive relations: $\vec{D} = {}_{0r}\vec{E}$, $\vec{B} = \mu_0\mu_r\vec{H}$, where ${}_r$ and μ_r are, for isotropic and homogeneous materials, two complex frequency-dependent parameters.

During recent decades, a great variety of novel and complex materials have been designed with promising practical applications. It has been found, however, that in many cases the relations between electric and magnetic fields cannot be described by standard constitutive equations. Among these new materials we may mention, for example, chiral, nonreciprocal, gyrotropic and negative refractive index media. Bi-isotropic media are the most general linear, homogeneous and isotropic materials, and they respond to electromagnetic excitation according to the following relations:

$$\begin{aligned} \vec{D} &= {}_{0r}\vec{E} + (\chi - j\kappa)\sqrt{{}_0\mu_0}\vec{H} \\ \vec{B} &= \mu_0\mu_r\vec{H} + (\chi + j\kappa)\sqrt{{}_0\mu_0}\vec{E} \end{aligned} \tag{1}$$

where κ is the chirality, a dimensionless parameter for describing the handedness of the material, and χ is the Tellegen parameter, a dimensionless quantity for the degree of inherent nonreciprocity in the medium [1]. The reciprocal chiral medium, also known as Pasteur medium, is a class of bi-isotropic medium characterized by $\chi = 0$. The electromagnetic behavior of these materials reflects two effects: electromagnetic rotatory dispersion, which causes a rotation of the polarization direction for a linearly polarized wave, and circular dichroism (a

change in the polarization from linear to elliptical) due to the different absorption coefficients of right- and left-handed circularly polarized waves.

Electromagnetic activity at optical frequencies was first observed in the XIX century, [2, 3]. Although nature presents many examples of chiral media at optical frequencies, there is, to the best of our knowledge, no natural medium able to produce electromagnetic activity at microwave frequencies. At these frequencies, the first man-made chirals were manufactured by embedding a random distribution of conducting helices with the same handedness into a host medium. The first experimental studies were developed using basic free-wave systems with the aim of verifying electromagnetic activity at microwave frequencies. Lindman [4] and later Tinoco and Freeman [5] found a critical wavelength for copper helix at $\lambda \cong 2L$, where L is the length of the wire in the helix; this constitutes a rule of thumb to select the frequency range in which to search for interesting effects. By far, the most used structure for chiral manufacture has been the metallic helix [6-10], although other elements such as metallic cranks have also been used [11]. Manufacturing techniques have evolved from the random inclusion of metallic particles to the presently used alternatives, which are based on periodic distribution of planar or quasi-planar chiral particles printed on a circuit board or even integrated circuits. The interested reader can find a review in [12].

The ordered distribution of resonant structures in a periodic lattice enhances the electromagnetic effects and is able to produce larger electromagnetic activity and circular dichroism. These enhanced chirals are often known as chiral metamaterials. It has been found that a material with very high electromagnetic activity can also possess a negative refractive index [13]. During the last decade, a large variety of resonant structures have been designed and analyzed in order to produce high values of optical activity, circular dichroism and negative refractive index; for example, see [14-15] and references therein.

The presence of the chirality parameter in the constitutive equations prevents the use of standard characterization procedures. Furthermore, the existence of resonant structures, which finally produce strong variations in the characteristic parameters, makes the retrieval algorithms more complicated. In this paper, the main techniques for chiral characterization are reviewed. The second section is devoted to free-wave methods, which are the most widely used systems for chiral characterization. The guided methods presented in the third section, usually provide more accuracy than the free-wave methods, although the search for electromagnetic rotatory dispersion limits the guided systems to those of axial symmetry. In section four, resonator techniques are considered. Finally, the accuracy and feasibility of each technique is discussed.

2. Electromagnetic fields in chiral media

The constitutive relations (1) for reciprocal media ($\chi = 0$), are:

$$\begin{aligned} \vec{D} &= \varepsilon_0 \varepsilon_r \vec{E} - j\kappa / c \vec{H} \\ \vec{B} &= \mu_0 \mu_r \vec{H} + j\kappa / c \vec{E} \end{aligned} \tag{2}$$

http://dx.doi.org/10.5772/51539

where $c=(_0\mu_0)^{-1/2}$. The rotational Maxwell equations present a coupling between the electric and magnetic fields. In frequency domain and for the sourceless case, the curl of the electric and magnetic fields are:

$$\begin{aligned} \nabla \times \vec{E} &= - j\omega\left(\frac{j\kappa}{c}\vec{E} + \mu\vec{H}\right) \\ \nabla \times \vec{H} &= j\omega\left(\vec{E} - \frac{j\kappa}{c}\vec{H}\right) \end{aligned} \tag{3}$$

It is possible to find a linear combination of the E and H fields, called normal modes and written $\{\vec{E}^n,\ \vec{H}^n\}_{n=1,2}$, that satisfy independent rotational Maxwell equations so that:

$$\left\{\begin{array}{l} \nabla \times \vec{E}^n = - j\omega\mu^n\vec{H}^n \\ \nabla \times \vec{H}^n = j\omega^n\vec{E}^n \end{array}\right\}_{n=1,2} \tag{4}$$

These combinations of electromagnetic fields propagate through the chiral material as through an isotropic non-chiral medium, with equivalent constitutive parameters: $\{^n,\ \mu^n\}_{n=1,2}$.

The normal modes satisfying eq. (4) are:

$$\begin{aligned} \vec{E}^1 \equiv \vec{E}_+ &= \frac{1}{2}(\vec{E} - j\eta\vec{H}), \quad & \vec{H}^1 \equiv \vec{H}_+ &= \frac{j}{\eta_+}\vec{E}_+ \\ \vec{E}^2 \equiv \vec{E}_- &= \frac{1}{2}(\vec{E} + j\eta\vec{H}), \quad & \vec{H}^2 \equiv \vec{H}_- &= \frac{-j}{\eta_-}\vec{E}_- \end{aligned} \tag{5}$$

the medium parameters being:

$$\begin{aligned} _\pm &= (1 \pm \kappa_r) \\ \mu_\pm &= \mu(1 \pm \kappa_r) \end{aligned} \tag{6}$$

where $\kappa_r = \kappa \Big/ \sqrt{_r\mu_r}$ is the relative chirality, and:

$$\eta = \eta_\pm = \sqrt{\mu_\pm / _\pm} = \sqrt{\mu / } \tag{7}$$

2.1. Plane wave propagation in chiral media

A propagating wave can always be expressed as a linear combination of the propagation of normal modes. The propagation constant for each mode $\{\vec{k}_+, \vec{k}_-\}$ could be, in principle, different:

$$\begin{aligned}\vec{E}_{\pm}(\vec{r}) &= \vec{E}_{\pm} exp\left(-j\vec{k}_{\pm} \bullet \vec{r}\right) \\ \vec{H}_{\pm}(\vec{r}) &= \vec{H}_{\pm} exp\left(-j\vec{k}_{\pm} \bullet \vec{r}\right)\end{aligned} \tag{8}$$

If the wave is propagating in the $\hat{u}$ direction, the modes propagation constants are:

$$\vec{k}_{\pm} = \hat{u} k_{\pm} \tag{9}$$

where $k_{\pm} = \omega\sqrt{\pm\mu_{\pm}} = \omega\sqrt{\mu}(1 \pm \kappa_r) = \omega\, n\, (1 \pm \kappa_r) \big/ c$. The refraction indices for each mode are

$$n_{\pm} = n(1 \pm \kappa_r) \tag{10}$$

It can be deduced, from eq. (4, 5), that the vectors $\hat{u}$, $\vec{E}_{+}$ and $\vec{H}_{+}$ are mutually orthogonal. And the same happens to $\hat{u}$, $\vec{E}_{-}$ and $\vec{H}_{-}$. Also, according to eq. (5) the propagation modes are circularly polarized electromagnetic waves to the right (RCP) $\{\vec{E}_{+}, \vec{H}_{+}\}$ and to the left (LCP) $\{\vec{E}_{-}, \vec{H}_{-}\}$.

3. Free-wave

3.1. Experimental systems

For regular materials where and μ are the only parameters to be retrieved, the experimental determination of the complex scattering coefficients S_{11} and S_{21} are sufficient to solve the problem. But there remains an extra parameter to be determined, the chirality κ. To do this, we are forced to experimentally measure one complex or two real additional quantities. This is usually achieved in terms of the reflection coefficient and the two transmission coefficients corresponding to the parallel and perpendicular direction to the incident wave. Sun et al. [16] measured the complex reflection coefficients of short-circuit (backed with metal) and open-circuit (not backed with metal) samples. For transmission, they measured the rotation angle and the axial ratio.

The usual free-wave experimental setup consists of a pair of transmitting and receiving antennas, a sample holder, a vector network analyzer (to determine magnitude and phase of the scattering parameters) and a calibration kit. In order to minimize the diffraction effects at the edges of the sample it is necessary to decrease the size of the beam or place the sample close to the antennas. But if the antenna is close to the sample, the conditions of plane wave are not accomplished and the far-field retrieval algorithms cannot be applied. Moreover, the effects of multiple reflections between the antenna and the sample are enhanced, which introduces extra errors into the measurements. The size of the beam can be reduced by placing focusing devices, such us spot focusing lens in the antennas [17] or an ellipsoidal reflector mirror after the transmitting antenna [18]. Behind the focus, the wave is not plane, but takes

http://dx.doi.org/10.5772/51539

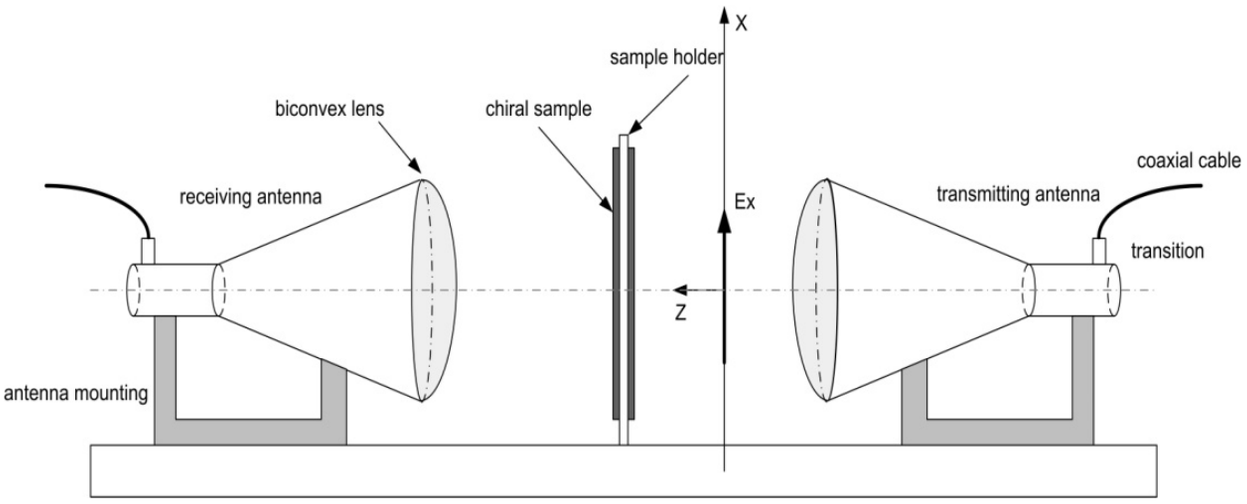

Figure 1. Setup for free-wave measurement, modified from [6, 17, 21].

the configuration of a Gaussian beam. In this case, the plane wave assumption does not introduce serious errors in the measurements [19].

Figure 1 shows a schematic diagram of the experimental system developed by Varadan et al. [6, 17, 20]. It makes use of a lens in each antenna to focus the wave; the sample is located in the common focal plane. The transmitting and receiving antennas are mounted on a carriage and the distance between them can be adjusted for calibration. This setup was initially developed by Ghodgaonkar [21] to measure permittivity and permeability, and later adapted to determine rotation angle, ellipticity and power absorption. Making use of this system, Guire et al. [20] measured the normal incidence reflection of linearly polarized waves of metal-backed chiral composite samples at microwave frequencies. Ro et al. [6], determined the ellipticity, rotation angle and power absorption for samples containing helix and observed that, at resonance, the angle of rotation rapidly increases or decreases or even changes its sign, a phenomenon also known as the Cotton effect. They also reported that this phenomenon is observed in the frequency region where maximum electromagnetic power absorption occurs.

Figures 2 and 3 show a picture and a schematic diagram, respectively, of the free-wave experimental system developed by the authors. The setup is based on a previous one for permittivity and permeability measurements [22], and adapted to measure electromagnetic activity [10]. This system has been used to characterize chiral materials based on random distribution of elements and periodical lattices [10-11, 23-25].

The incident beam is focused by an ellipsoidal concave mirror, with the transmitting antenna placed at one of the mirror foci and the sample at the other. The position of the receiving antenna is not crucial in this configuration. Figure 2 shows a diagram where the focusing mirror and sample holder are not shown for clarity. The incident wave is linearly polarized in the x-axis direction. The rotation on the polarization angle, θ, is defined as the difference between the polarization direction of the incident wave and the direction of the major axis of the transmitted elliptically polarized wave.

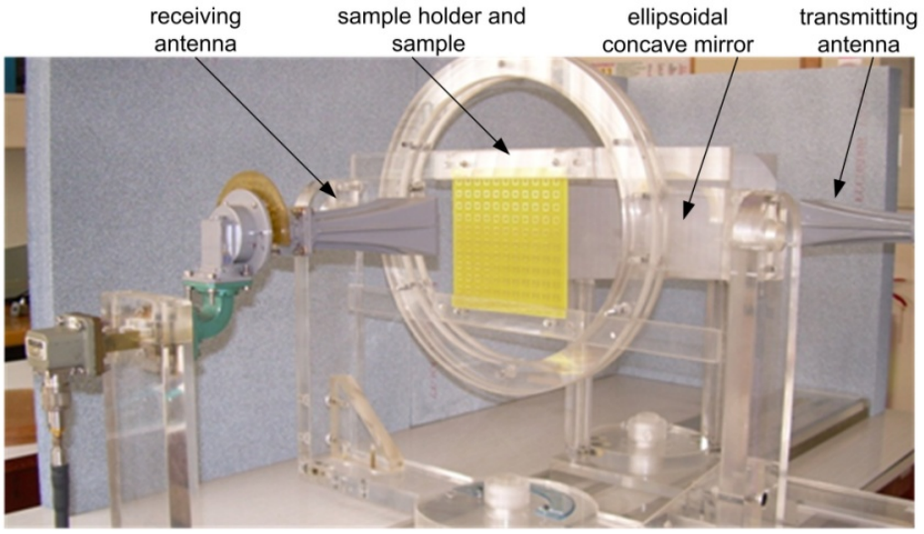

Figure 2. Photo of the free-wave setup in the X-band developed by the authors.

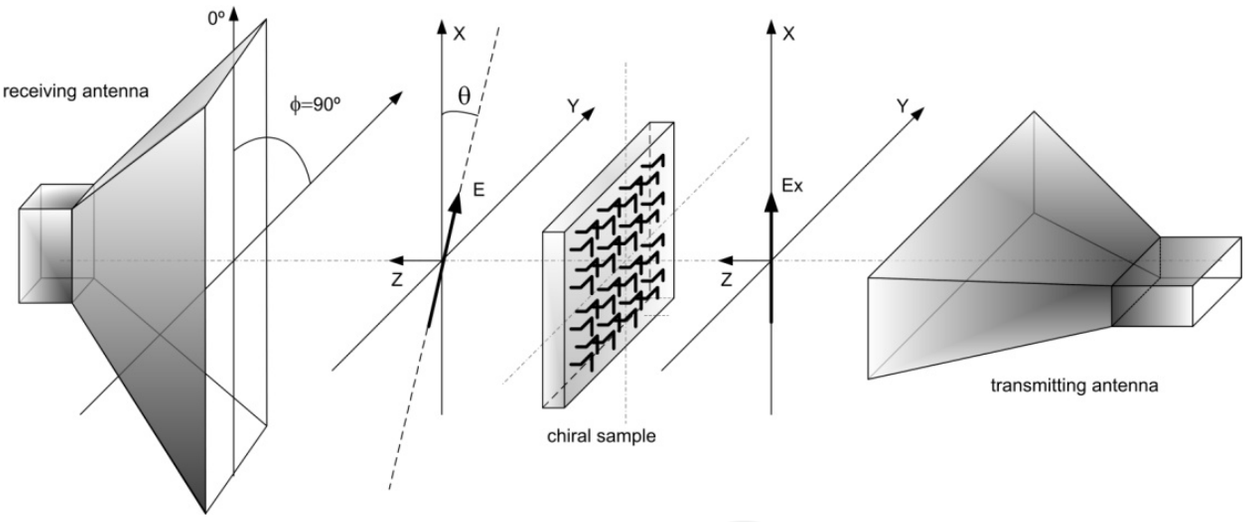

Figure 3. Schematic diagram of figure (2), where the receiving antenna with a rotation angle of 90° to measure T_{CR}. The focusing mirror and sample holder are not shown for clarity.

The experimental system presented by Wang et al. [14] to characterize chiral metamaterials with high electromagnetic activity makes use of a pair of standard gain horn antennas, which are located close to the sample, without any focusing device. This configuration leads to multiple reflections and border diffractions, which affect the experimental reflection and transmission coefficients.

The scattering parameters are measured using a vector network analyzer. First, a two port calibration should be made, for which purpose the TRL (Transmission, Reflection, Line) technique is one of the most frequently used. The basic TRL calibration process is a two port calibration widely used in non-coaxial environments, such as waveguide and free-wave

systems[1]. TRL uses a 12-term error model with three calibration standards: THRU, REFLECT and LOAD. For the THRU step, the test ports are connected and the four S-parameters are measured in both directions. For the REFLECT step, a highly reflective device is connected to each port and the reflection coefficients are measured. In the LINE step, a short transmission line is inserted and, again, the four S-parameters are measured.

The reference planes of the calibration can be located at the sample surface [17] or elsewhere, for example, at the two waveguide flanges where the antennas are connected [22]. In the first case, Ghodgaonkar et al. [17, 21] implemented the TRL calibration for free-wave systems: The THRU standard was configured by keeping the distance between the two antennas equal to twice the focal distance, without the sample. The LINE standard was achieved by separating the focal plane of transmitting and receiving antennas by a distance equal to a quarter of the free space wavelength at the center of the band. The REFLECT standards for both ports were obtained by placing a metal plate in the focal planes of the transmitting and receiving antenna, respectively.

The second option is the one used by the authors. In this case, it is possible to use standards for calibration in rectangular waveguide: a short-circuit is located at the antenna flanges for the REFLECT standard and a rectangular guide of $\lambda/4$ length for the LINE standard. A second calibration is necessary to shift the reference planes to the sample surface. To do that, the reflection coefficient, with a metal plate in sample position, and the transmission coefficient without the sample were used as reference measurements. Then, the ratio between the measurement with and without sample provides the magnitude of the scattering parameters of the sample. The phase of the reflection coefficient must be corrected by a π factor introduced by metal plate. For the phase of the transmission coefficient, it is necessary to subtract a quantity equals to $k_0 L$, where k_0 is the vacuum propagation constant and L is the sample width.

At first sight, the second TRL calibration option seems more complicated; however, it has the advantage of using LINE and THRU standards in rectangular waveguide, which are more accurate and easier to use than standards obtained by moving the antennas.

A time domain (TD) transform can be used to filter out mismatches from the antennas, edge diffraction effects and unwanted reflections from antennas, sample, mirrors or elsewhere. The network analyzer makes measurements in the frequency domain, and the time domain response is obtained by applying an inverse Fourier transform. The unwanted signals, which have longer paths than the direct signal, are separated from the main signal in the TD response and then can be removed by gating the signal. In order to obtain good filtering, it is necessary to clearly identify the sample response in the time domain and to choose the most suitable filter parameters [26]. The Fourier transform of the gated time-domain response provides the filtered signal. As will be shown later, this gating process greatly improves the experimental results.

1 Agilent Technologies Inc. Applying Error Correction to Network Analyzer Measurements, Application Note 2002, 1287-3, 5965-7709E.

3.2. Retrieval algorithm

The standard retrieval procedure for a normal medium relates the transmission and reflection coefficients with the electromagnetic properties of the medium. As mentioned above, for a chiral material a new experimental quantity is necessary. Here reflection coefficient, *R*, and the transmission coefficients parallel (co-polar, T_{CO}) and perpendicular (cross-polar, T_{CR}) to the polarization direction of the incident wave are the experimental data.

Consider a chiral slab of thickness *L*, which is illuminated by a normally incident linearly polarized plane wave $E_0\hat{x}$, Figure 4.

The incident wave may be decomposed as :

$$E_0\hat{x} = \frac{E_0}{2}(\hat{x} - j\hat{y}) + \frac{E_0}{2}(\hat{x} + j\hat{y}) \tag{11}$$

The reflected wave in z=*0* is $RE_0\hat{x}$, the co-polar and cross-polar transmitted fields in z=*L* are $T_{CO}E_0\hat{x}$ and $T_{CR}E_0\hat{y}$, respectively.

The reflected and transmitted electric fields are,

$$\vec{E}_r = \frac{1}{2}R_R E_0(\hat{x} - j\hat{y}) + \frac{1}{2}R_L\ E_0(\hat{x} + j\hat{y}), \tag{12}$$

$$\vec{E}_t = \frac{1}{2}T_R E_0(\hat{x} - j\hat{y}) + \frac{1}{2}T_L\ E_0(\hat{x} + j\hat{y}), \tag{13}$$

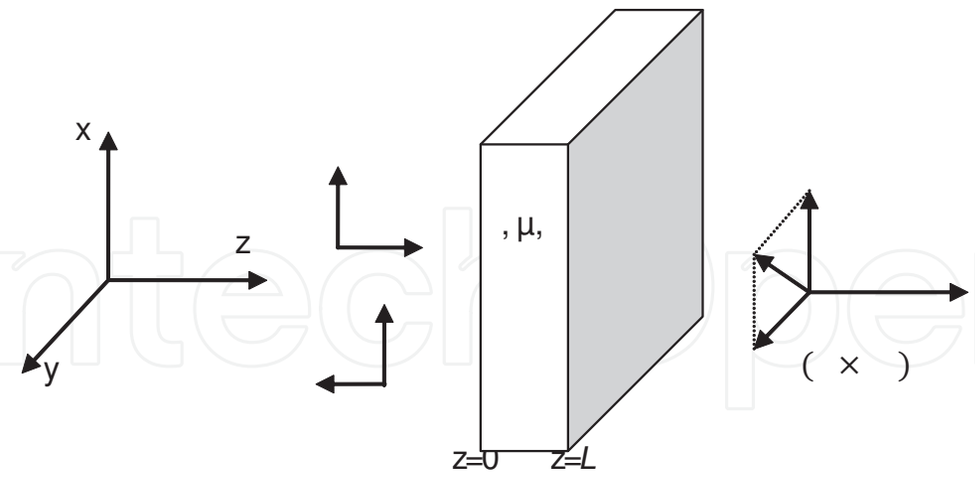

Figure 4. Schematic diagram of the experimental transmission and reflection coefficients and field of a chiral slab, where $\vec{E}_i$, $\vec{E}_r$ and $\vec{E}_t$ are the incident, reflected and transmitted fields, respectively.

where the subscript *R* (*L*) refers to right-hand (left-hand) circular polarization and subscript r to the reflected wave. The magnetic field can be expressed in a similar way in terms of wave impedance.

Applying the condition of continuity of tangential electric and magnetic fields at z=*0* and z=*L*, the reflection coefficients for RCP and LCP waves can be expressed as:

$$R_R = R_L = -\frac{j}{2}\frac{\sin(nk_0L)(1-\eta_r^2)}{2\eta_r\cos(nk_0L)+j(\eta_r^2+1)\sin(nk_0L)} \tag{14}$$

The experimental reflection coefficient is $R = R_R + R_L$. The transmission coefficients for the RCP and LCP waves are

$$T_R = \frac{2\eta_r e^{-j\kappa k_0 L}}{2\eta_r\cos(nk_0L)+j(\eta_r^2+1)\sin(nk_0L)} \tag{15}$$

$$T_L = \frac{2\eta_r e^{+j\kappa k_0 L}}{2\eta_r\cos(nk_0L)+j(\eta_r^2+1)\sin(nk_0L)} \tag{16}$$

These are related with the experimental transmission coefficients T_{CO} and T_{CR} by:

$$T_{CO} = \frac{1}{2}\left(T_R + T_L\right) \tag{17}$$

$$T_{CR} = \frac{-j}{2}\left(T_R - T_L\right) \tag{18}$$

It is useful to consider the following additional parameters:

$$T^2 \equiv T_R T_L \tag{19}$$

$$\Gamma \equiv -\frac{(T^2 - R^2 - 1) \pm \sqrt{(T^2 - R^2 - 1)^2 - 4R^2}}{2R} = \frac{\eta_r^2 - 1}{(\eta_r + 1)^2}\,, \tag{20}$$

$$P^2 = e^{-2jnk_0L} = \frac{R - \Gamma}{R\Gamma^2 - \Gamma} \tag{21}$$

We are now ready to compute the electromagnetic parameters. The relative impedance η_r is calculated from equation (20), where the correct sign in square root is selected according to $\mathrm{Re}(\eta) > 0$.

The refractive index is obtained from equation (21) and is:

$$n = j\frac{c}{4\pi fL}\ln|P^2| - \mathrm{Phase}(P^2)\frac{c}{4\pi fL} - \frac{c}{2fL}m \tag{22}$$

where *m* is an integer related to the branch index of the logarithm function. Only the imaginary part of *n* is unequivocally determined, but ambiguity arises for the real part because an infinite

number of solutions exist for different choices of m. The value of m can be determined by applying Kramers-Kronig relations to the wavenumber [28] or by expanding equation (22) in a Taylor series [29].

From n and η_r permittivity and permeability can be obtained:

$$_r = \frac{n}{\eta_r} \tag{23}$$

$$\mu_r = n\ \eta_r \tag{24}$$

The chirality parameter is obtained from T_L and T:

$$\frac{T_L}{T} = e^{\ j(\kappa k_0 L\ )} \quad \kappa = \frac{-j}{k_0 L} ln\left|\frac{T_L}{T}\right| + \frac{1}{k_0 L} Phase\left(\frac{T_L}{T}\right) + \frac{2\pi}{k_0 L} p \tag{25}$$

where p is an integer that can be determined by assuming null chirality far from resonance, continuity conditions, and that both real and imaginary parts resonate at the same frequency.

The retrieval procedure may fail and problems arise when the thickness L of the effective slab is not estimated accurately [30], when S_{11} and S_{21} are very small in magnitude [31] or when the first boundary of the effective homogeneous slab is not well determined [29]

The rotation angle θ and the ellipticity φ of the transmitted wave can be calculated by:

$$\theta = \frac{1}{2} arg\left(\frac{T_R}{T_L}\right), \tag{26}$$

$$\varphi = \frac{1}{2} tan^{-1}\left(\frac{|T_R|^2 - |T_L\ |^2}{|T_R|^2 + |T_L\ |^2}\right). \tag{27}$$

3.3. Results

As already mentioned, periodical structures provide certain advantages over random distributions: for example, they are easier to manufacture and are more homogeneous and they present extreme values for the rotation angle and chirality parameter. Figure 5 shows the reflection and transmission coefficients, and the retrieved parameters $_r$, μ_r, and κ_r, for a typical chiral slab composed of a periodical lattice of conductive cranks printed on a circuit board substrate. The dimensions of the crank are similar to those proposed by [23, 24]. Experimental measurements without and with TD filtering are shown in the first and second columns, respectively. The third column shows the results obtained through simulations based on the finite-difference time-domain method (FDTD). It can be seen that the TD filtering eliminates ripples in the measured transmission and reflection coefficients, which are usually associated with multiple reflections or residual post calibration errors.

A clear resonance at around 11 GHz is present in all the plots, both measured and simulated. Below the resonance, the retrieved parameters correspond to the blank FR4 board, which does not present electromagnetic activity ($_r$~4.2, μ_r~1.0). As the frequency approaches the resonance, all the parameters increase, with a maximum chirality in the order of κ~2.5. At resonance, the chirality changes the sign and its imaginary part peaks. The frequency dependence of permittivity and permeability observed in the plot are the same as those in metamaterials with a negative refractive index [14, 15, 24, 25]. The chirality parameter depends on frequency, which follows a Condon model for a homogeneous chiral medium [32].

There is good agreement between the retrieved parameters obtained from experiments with TD filtering and simulated data. It is important to highlight that the correct selection of TD parameters is crucial for obtaining good results in the retrieval process. The values of the time width (span) of the gating and the window shape affect the final results and, in this respect, the use of experimental and numerical data improves the calculations. Two propagation modes with two different velocities inside the chiral slab can be observed in the signal received by the receiving antenna when TD is applied, specially when the TCR coefficient is measured. Two Gaussian curves arrive at two different times, which implies a time span greater than that used for standard dielectric material.

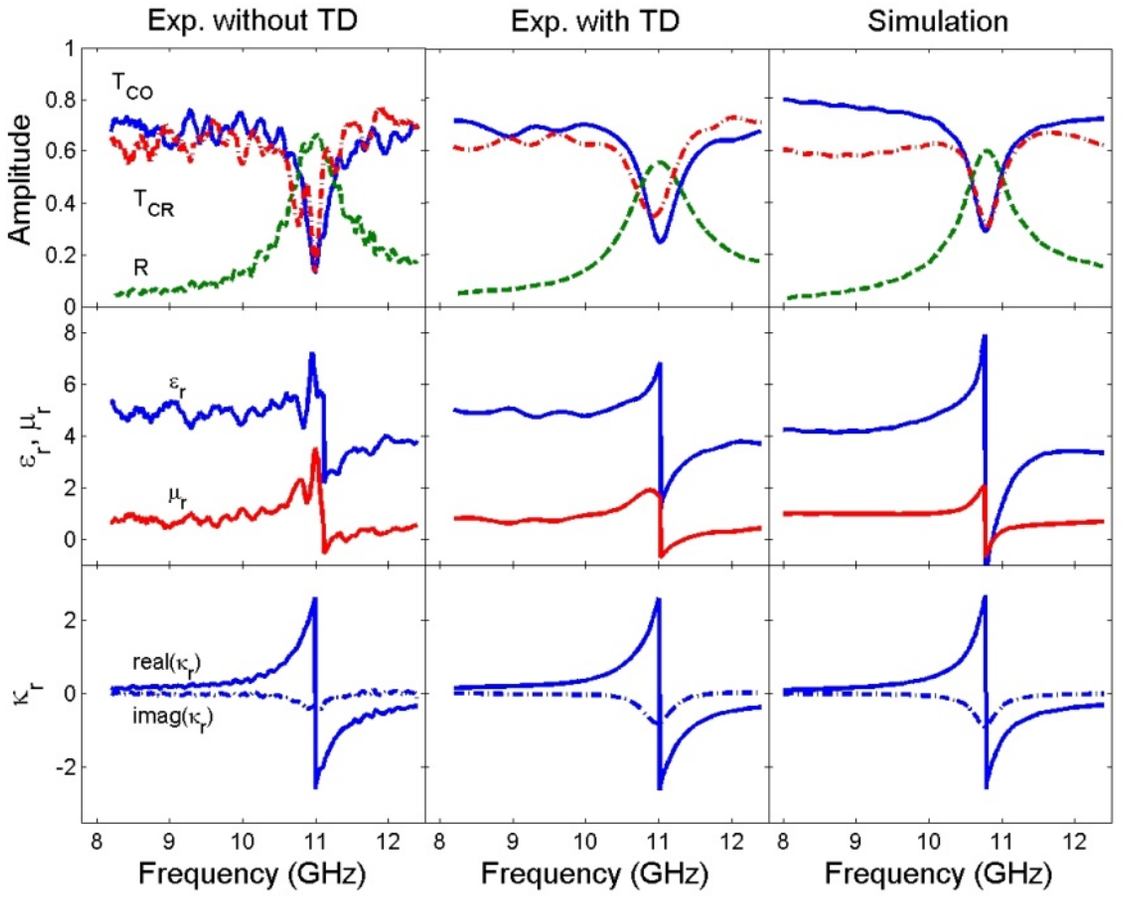

Figure 5. Transmission and reflection amplitudes (top panel), retrieved values for permittivity and permeability (middle panel) and chirality (bottom panel). Experimental results without time domain filtering are shown in the left column, with time domain filtering in the middle and simulation on the right.

4. Waveguides

4.1. Experimental systems

Waveguide techniques for characterizing chiral media are based on the same principles as free-wave techniques, and it is necessary to measure three complex quantities. The experimental setup, therefore, must allow measurements in, at least, two different polarizations for the transmission wave. All the experimental systems reported in the literature [7-9, 33-35] use circular waveguides because in rectangular waveguides the effects related to rotatory dispersion cannot be observed. Lubkowski [36] proposed a square waveguide for measurements with SRR (Split Ring Resonators). There, the orthogonal modes TE_{10} and TE_{01} are degenerated and, therefore, allow propagation for co-polar and cross-polar polarization. This could be a good alternative for measurement involving chiral materials but, to the best of our knowledge, such a system has not been implemented experimentally.

Figures 6 and 7 show a picture and a schematic diagram, respectively, of the experimental setup using a circular waveguide developed by the authors. It is similar to that used by Brewitt-Taylor [7] et al. and Liu et al. [34]. The circular measurement cell containing the chiral sample (2 in Figures 6, 7) is fed with a linearly polarized wave through a rectangular-to-circular waveguide transition (1 in Figures 6, 7). The transmission wave passes to the rectangular waveguide through another transition which can rotate around the longitudinal axis (3 in Figures 6, 7), enabling measurements in different polarizations. The waveguide transition contains a section of resistive film to absorb any field cross-polarized from the fields being measured, which prevents them from being reflected from the waveguide transition back on to the sample.

S-parameters are measured using a network analyzer and the TRL technique is used for calibration as described for free-wave measurements. The REFLECT standard is achieved by shorting with a metal plate the flanges where the measurement cell is connected, which defines the reference planes. The TRHU standard is achieved simply by connecting directly these flanges without the measurement cell. Finally, the LINE standard is a section of the circular waveguide quarter wavelength at midband.

Hollinger et al. [33] measured some effects of chiral materials including rotatory dispersion and circular dichroism, but they did not study the inversion procedure. Liu et al. [9, 34] used a slotted line instead of the network analyzer to measure the reflection coefficients of short-circuited and open-circuited samples, completing the experimental measurements with the rotation angle and axial ratio. Reinert et al. [8, 35] used coaxial-to-circular waveguide transition to excite the fundamental mode in circular waveguide TE_{11}, avoiding rectangular-to-circular transitions.

Two aspects that can produce important errors must be taken into account in waveguide measurements: the presence of local density variations in the sample, which causes fluctuations to the measurements, depending on sample orientation, and the existence of gaps between the sample and the waveguide walls. In order to improve the accuracy of the results, the samples are rotated and the measured scattering parameters for several positions are averaged in an attempt to overcome the sample variations and inhomogeneities [8, 9, 33, 34]. The influence of the gap depends on sample manufacturing and can be overcome, for instance, by locating the chiral particles in non-conducting spheres [8], since the multiple air gaps between the spheres are part of the sample, or by using an elastic material as dielectric host for distributing the chiral particles [12].

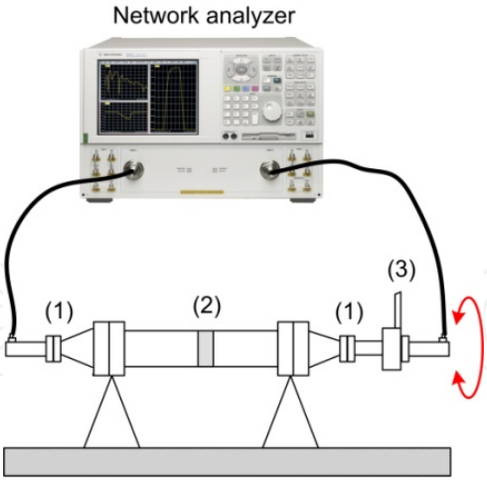

Figure 6. Schematic diagram of the X-band circular waveguide experimental system developed by the authors.

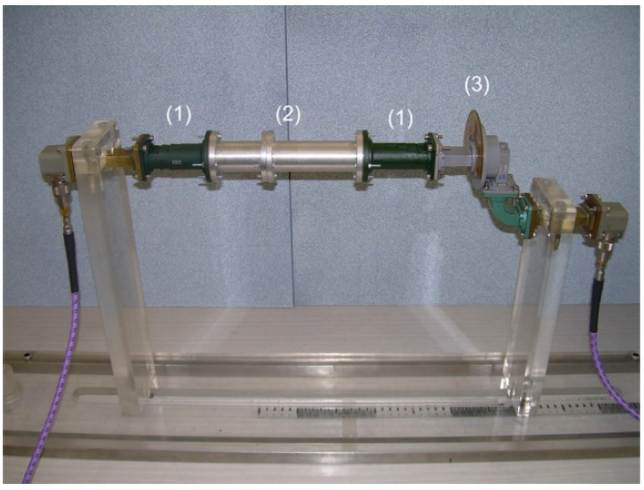

Figure 7. Photo of the experimental diagram of Figure 6.

4.2. Modes in circular waveguides

The propagation of electromagnetic fields in circular waveguides filled with chiral media, also known as chirowaveguides, can be better understood by using the normal modes formulation. Assuming, as usual, solutions of the type $e^{-\gamma z}$, the longitudinal component of the electric field satisfies the Helmholtz equation [37],

$$\left(\nabla_t^2 + K_\pm^2\right)E_{\pm z} = 0, \tag{28}$$

where $K_\pm = \left(k_\pm^2 - \gamma^2\right)^{1/2}$.

Once $E_{\pm z}$ are known, the transversal components can be obtained by:

$$E_t(\vec{r}) = \frac{1}{K_+^2}(-\gamma \nabla_t - k_+ \hat{z} \times \nabla_t) E_{+z} + \frac{1}{K_-^2}(-\gamma \nabla_t - k_- \hat{z} \times \nabla_t) E_{-z} \tag{29}$$

Similar expressions for the magnetic components can be deduced. Assuming an azimuthal dependence as $e^{-jm\varphi}$, the longitudinal component of the electric field is a linear combination of the longitudinal components of the normal modes:

$$E_z(\vec{r}) = \sum_{m=-\infty}^{\infty} \sum_{l=1}^{\infty} \{A_{m,l,+} J_m(K_{l,+}\rho) + A_{m,l,-} J_m(K_{l,-}\rho)\} e^{-jm\varphi} e^{-\gamma_l z} \tag{30}$$

where classification of the normal modes is described by $\{m, l\}$ indices. $A_{m,l,\pm}$ is the amplitude of the mode, J_m is the m order Bessel function and J'_m its derivate. If the boundary is ideally conducting, the following eigenvalue equation is obtained:

$$\frac{m\gamma_l}{a}\left(\frac{1}{K_{l,+}^2} - \frac{1}{K_{l,-}^2}\right) + \frac{k_+}{K_{l,+}^2}\frac{J'_m(K_{l,+}a)}{J_m(K_{l,+}a)} + \frac{k_-}{K_{l,-}^2}\frac{J'_m(K_{l,-}a)}{J_m(K_{l,-}a)} = 0 \tag{31}$$

where a is the waveguide radius. For a pair of solutions satisfying $\gamma_{l'} = -\gamma_l$ and $m' = -m$, the parameters K_+ K_- are coincident. The wave number is, in general, a complex quantity $\gamma_l = \alpha_l + j\beta_l$.

Figure 8 shows the dispersion diagram of a circular waveguide for X band (a=1.19cm) filled with a chiral material ($\varepsilon_r = 3.0$, $\mu_r = 1.0$, κ_r=0.8) for $m = \pm 1$. This diagram is, clearly, much more complex than the one corresponding to a non-chiral waveguide. A detailed discussion on the modal expansion can be found in [37].

4.3. Retrieval algorithm

When several modes propagate in the chirowaveguide it is not possible to obtain inverse equations. Only if just one mode propagates can a simple retrieval algorithm be developed. However, this is only valid for low values of the chirality parameter.

Liu et al. [9, 34] assumed that only the fundamental mode, $HE_{\pm 11}$ ($m = \pm 1$, j=1), propagates in the sample, and this is approximately treated in the same way as the TE_{11} mode, the fundamental mode in the empty waveguide. In this case, the procedure for obtaining the inversion equations is similar to the one used in the free-wave technique. The above mentioned authors used the following experimental quantities: Γ_1 and Γ_2, the complex reflection coefficients of the open circuit sample (sample in transmission situation) and the short circuit sample (sample backed with metal plate) in the circular waveguide, respectively, θ is the rotation angle and R_A is the axial ratio, for the electromagnetic waves travelling through chiral material in the circular waveguide.

The characteristic parameters of the material are calculated from the measured quantities by:

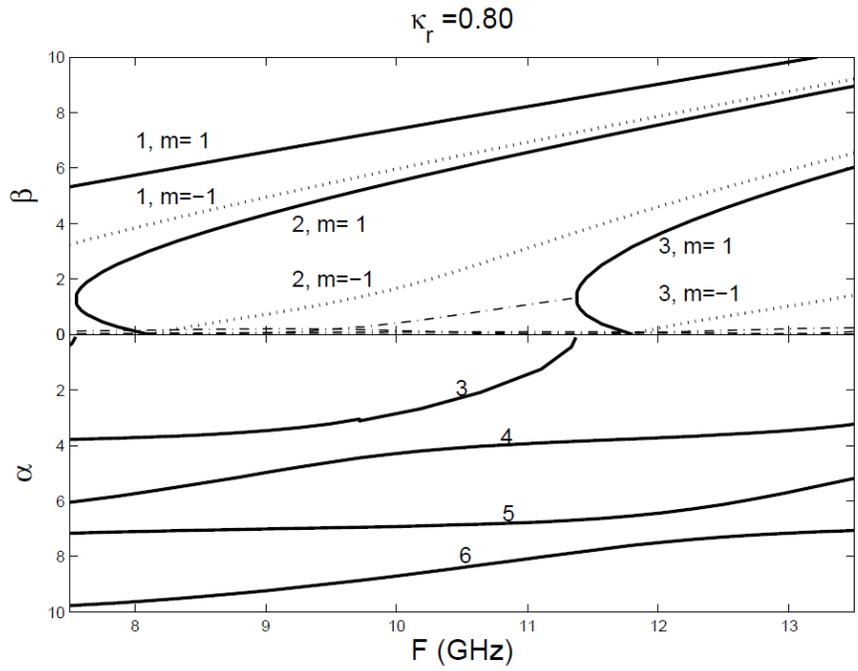

Figure 8. Dispersion diagram of chirowaveguide (1.19 cm radius, $_r = 3.0$, $\mu_r = 1.0$, $\kappa_r = 0.8$), for $m = 1$ (solid line), $m = -1$ (dotted line). The propagation constant at frequencies below the cut-off is shown by dash-dot lines.

$$Z_0' = \frac{\omega \mu_0}{\left[\omega^2{}_0 \mu_0 - k_c^2\right]^{1/2}} \tag{32}$$

$$Z_\omega = Z_0' \left(\frac{\Gamma_1 \Gamma_2 + \Gamma_1 + \Gamma_2 + 1}{\Gamma_1 \Gamma_2 - 3\Gamma_1 + \Gamma_2 + 1} \right)^{1/2} \tag{33}$$

$$A = \frac{1}{2d} arccos\left(\frac{\Gamma_1 \Gamma_2^2 + \Gamma_2^2 - 2\Gamma_1 \Gamma_2 - \Gamma_1 + 1}{2(\Gamma_1 - \Gamma_2)} \right) \tag{34}$$

$$B = \frac{1}{2d} \left(2\theta - j \tanh^{-1} \frac{2R_A}{1 + R_A^2} \right) \tag{35}$$

$$\mu = \frac{Z_\omega A}{\omega} \tag{36}$$

$$\kappa = \frac{B\left(A^2 + k_c^2\right)^{1/2}}{a \mu \omega} \tag{37}$$

$$= \frac{\left(A^2 - B^2\right) \mu \kappa^2}{B^2} \tag{38}$$

where d is the thickness of the chiral sample and k_c the cut-off constant for the fundamental mode TE_{11} in the empty waveguide.

These equations are relatively easy to use but are only valid for media with small values of the characteristic parameters. For example, Figure 8 shows two propagating modes in the X-Band for a chirality relative constant κ_r=0.8, and, so, the previous retrieval algorithm would not be useful in that case. Other authors consider more modes. For instance, Busse et al. [8, 35] used five modes but could not find inversion equations to calculate the permittivity, permeability and chirality of the medium. Instead, they processed the direct problem numerically, in an iterative way, to fit measured quantities: the reflection coefficient R, the co-polar transmission coefficient T_{CO}, and the cross-polar transmission coefficient T_{CR}. Using the expression for waveguide modes in the empty and filled regions and starting with approximate values for permittivity, permeability and chirality, the material properties are obtained by iterative fitting of the calculated S parameters to the experimental ones.

Brewitt-Taylor et al. [7] followed a similar procedure to calculate the characteristic parameters. More specifically, they used four modes and eight different points to perform the modal analysis in the interfaces. In this case, mode matching was performed at the two interfaces simultaneously. The number of iterations required varied from 5 to 30, although the authors admit that high chirality samples could require more iterations.

Both Reinert et al. and Brewitt-Taylor et al. established the number of modes empirically, this number increasing with the values of the characteristic parameters. For instance, the samples used by Brewitt-Taylor et al. presented maximum values of 4 for the permittivity, 0.5 for the chirality and around 1 for the permeability, while the corresponding rotation angle was always less than 20º. Samples manufactured by the authors present values of up to 7 for permittivity, and 2 for chirality and permeability (see Figure 5), finding rotation angles in the range of 90º (Figure 9). The number of modes which should be used is, probably, more than five, increasing the computation requirements.

5. Resonators

Some authors propose using resonator techniques to characterize chiral media [38, 39]. Such techniques are usually the most suitable method for obtaining high precision measurements. However, there are several reasons why they are difficult to use with chiral media. In particular, resonators work at discrete frequencies this is not useful to deal with dispersive media; only two real quantities (resonant frequency and quality factor) can be measured and, as mentioned above, three complex quantities have to be measured to extract permittivity, permeability and chirality. Measurements using different resonant modes and samples in several positions is a possibility, but, in this case, the experimental procedure becomes very complicated.

Tretyakov et al. [38, 39] proposed a perturbation technique, although this gives rise to a new problem. It is well known that perturbation techniques are only valid for small samples. But

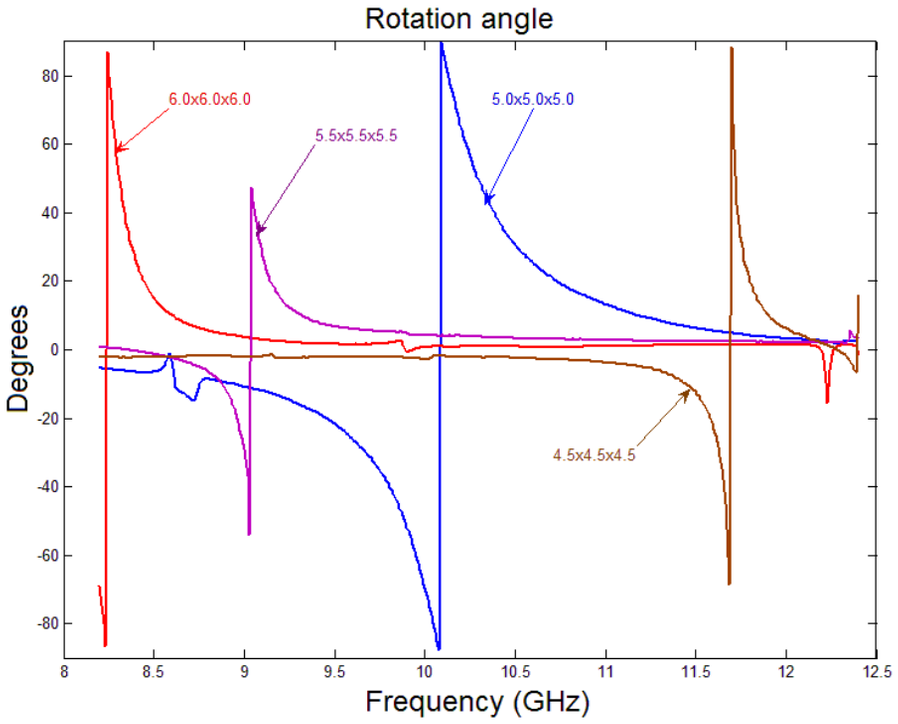

Figure 9. Rotation angle produced by several samples composed of four cranks in foam [12]. Labels indicate the size (in mm) of the cranks.

small samples of chiral media will have a small number of inclusions, perhaps only one, and so it makes no sense to treate them as a homogeneous material.

In our opinion, resonant techniques are not suitable for characterizing chiral media. In fact, although Tretyakov et al. studied the proposed technique theoretically, none was implemented experimentally.

6. Discussion and conclusions

In this work, microwave techniques for characterizing chiral media have been revised, and free-wave, waveguide and resonator techniques have been analyzed. Since chiral materials are characterized by three complex parameters, permittivity, permeability and chirality, at least, three experimental quantities have to be measured. All the techniques considered present some difficulties, while free-wave techniques are, in our opinion, the most suitable: i) They do not need any special component. ii) Quasi-plane wave propagation can be assumed in the sample, so that inversion equations for extracting characteristic parameters can be developed without difficulty. Usually, the measured quantities are the reflection coefficient, the co-polar and cross-polar transmission coefficients.

Free-wave methods present an inherent problem due to the finite size of the sample, which should be large enough to avoid diffraction at the borders. Several techniques found in the

literature overcome this problem by using focusing systems, lenses or ellipsoidal mirrors. They concentrate the propagated wave at a tiny spot, where the sample is situated and so reasonably sized samples can be used. Many authors use time domain transformations to remove unwanted reflections from the experimental measurements.

Waveguide measurements may be considered a possible alternative. The measuring principle is similar to that of free-wave techniques, but they present the advantage of avoiding many kinds of external interference and use only small samples, although good machining is needed. However, they present one serious problem: usually several modes are propagated in the sample and inversion equations cannot be developed. All the techniques found in the literature use a circular waveguide because axial symmetry is necessary for measurements in different polarizations (only waves with polarization parallel to the short side can be propagated in rectangular waveguide). Unfortunately many circular waveguide components are not commercially available. A common solution is to use a rectangular waveguide and to feed the measurement cell, made in the circular waveguide, by means of two rectangular to circular waveguide transitions. The transition contains a resistive film to absorb any fields cross-polarized from those being measured. Square waveguides could, in principle, be another alternative for chiral characterization, although we have not found any theoretical nor experimental study in the current literature.

Finally, it should be emphasized that resonator techniques are not suitable for characterizing chiral media. Only one research group has proposed a resonator technique in a theoretical study without experimental implementation. In fact, resonators work at a fixed frequency and are therefore not useful for measurements in dispersive media.

Acknowledgements

This work was supported by the Dirección General de Investigación (TEC 2010-21496-C03-02) of the Spanish Ministry of Education and Science and by Fundación Séneca (11844/PI/09) Región de Murcia (Spain).

Author details

J. Margineda[1], G. J. Molina-Cuberos[1], Núñez[1], A. J. García-Collado[1,2] and E. Martín[1]

1 Universidad de Murcia, Murcia, Spain

2 Universidad Católica San Antonio, Murcia, Spain

References

[1] Lindell, I. V, Sihvola, A. H, Tretyakov, S. A, & Vitanen, A. J. Electro-magnetic Waves in Chiral Media, Boston, USA: Artech House; (1994).

[2] Arago, D. F. Mémoire sur une Modification Remarquable Qu'éprouvent les Rayons Lumineux dans leur Passage a Travers Certains Corps Diaphanes, et sur Quelques Autres Nouveaux Phénoménes D'optique. Mémoires de la Classe des Sciences Mathématiques et Physiques de l'Institut Impérial de France (1811). , 1-93.

[3] Biot, B. Mémoire sur un Nouveau Genre D`Oscillation que les Molécules de la Lumiére Éprouvent en Traversant Certains Cristaux. Mémoires de la Classe des Sciences Mathématiques et Physiques de l'Institut Impérial de France (1812). , 1-1.

[4] Lindman, K. F. Om en Genom ett Isotropt System av Spiralformiga Resonatorer Alstrad Rotationspolarisation av de Elektromagnetiska Vagorna. Öfversigt af Finska Vetenskaps-Societetens förhandlingar, A. Matematik och naturvetenskaper (1914). LVII (3) 1-32.

[5] Tinoco, I, & Freeman, M. P. The Optical Activity of Oriented Copper Helices. I. Experimental, J Physical Chemistry (1957). , 61-1196.

[6] Ro, R, Varadan, V. V, & Varadan, V. K. Electromagnetic Activity and Absorption in Microwave Composites, Proc. Inst. Elect. Eng. H (1992). , 139(5), 441-448.

[7] Brewitt-taylor, C. R, Lederer, P. G, Smith, F. C, & Haq, S. Measurement and Prediction of Helix-Loaded Chiral Composites, IEEE Transactions on Antennas and Propagation. (1999). , 47(4), 692-700.

[8] Busse, G, Reinert, J, & Jacob, A. F. Waveguide Characterization of Chiral Material: Experiments. IEEE Transactions on Microwave Theory and Techniques (1999). , 47(3), 297-301.

[9] Sun, G, Yao, K, & Liu, Z. Influence of Helix Parameters on the Reflectance of Microwave by Chiral Composites, IEEE Transactions on Electromagnetic Compatibility (1999). , 411-350.

[10] Gómez, A, Lakhtakia, A, Margineda, J, Molina-cuberos, G. J, Núñez, M. J, Ipiña, S. A, & Vegas, A. Full-Wave Hybrid Technique for 3-D Isotropic-Chiral-Material Discontinuities in Rectangular Waveguides: Theory and Experiment, IEEE Transactions on Microwave Theory and Techniques (2008). , 56(12), 2815-2824.

[11] Molina-cuberos, G. J, García-collado, A. J, Margineda, J, Núñez, M, & Martín, E. Electromagnetic Activity of Chiral Media Based on Crank Inclusions, IEEE Microwave and Wireless Components Letters. (2009). , 19(5), 278-280.

[12] Barba, I. Cabeceira ACL, García-Collado AJ, Molina-Cubero GJ, Margineda J, Represa J. Quasi-planar Chiral Materials for Microwave Frequencies. In: Kishk A. (ed.) Electromagnetic Waves Propagation in Complex Matter, Intech

978-9-53307-445-0(2011). Available from: http://www.intechopen.com/books/electromagnetic-waves-propagation-in-complex-matter

[13] Pendry, J. B. A Chiral Route to Negative Refraction, Science (2004).

[14] Wang, B, Zhou, J, Koschny, T, Kafesaki, M, & Soukoulis, C. M. Chiral Metamaterials: Simulations and Experiments, J. Opt. A: Pure Appli. Opt. (2009).

[15] Mackay, T. G, & Lakhtakia, A. Negatively Refracting Chiral Metamaterials: A Review, SPIE Reviews (2012).

[16] Sun, G, Yao, K, Liu, Z, & Huang, Q. A Study on Measuring the Electromagnetic Parameters of Chiral Materials. J. Phys. D: Appl. Phys. (1998). , 31-2109.

[17] Chen, L F, Ong, C. K, Neo, C. P, Varadan, V. V, & Varadan, V. K. Microwave Electronics Measurement and Materials Characterization, Chinchester, England: John Wiley & Sons; (2004).

[18] Lynch, A. C, & Simkin, D. Measurement of Permeability and Permittivity Of Ferrites. Measurement Science Technology (1990). , 1-1162.

[19] Rickard Petersson LESmith GS. An Estimate of the Error Caused by the Plane-Wave Approximation in Free-Space Dielectric Measurement Systems, IEEE Transactions on Antennas Propagation. (2002). , 50(6), 878-887.

[20] Guire, T, Varadan, V. K, & Varadan, V. V. Influence of Chirality on the Response of EM Waves by Planar Dielectric Slabs, IEEE Transactions on Electromagnetic Compability. (1990). , 32(4), 300-303.

[21] Ghodgaonkar, D. K, Varadan, V. V, & Varadan, V. K. A Free-Space Method for Measurement of Dielectric Constants and Loss Tangent at Microwave Frequencies. IEEE Transactions on Instrumentation and Measurement. (1989). , 38-789.

[22] Muñoz, J, Rojo, M, Parreño, A, & Margineda, J. Automatic Measurement of Permittivity and Permeability at Microwave Frequencies Using Normal and Oblique Free-Wave Incidence with Focused Beam, IEEE Transactions on Instrumentation and Measurements. (1998). , 47(4), 886-892.

[23] García-collado, A. J, Molina-cuberos, G. J, Margineda, J, Núñez, M. J, & Martín, E. Isotropic and Homogeneous Behavior of Chiral Media Based on Periodical Inclusions of Cranks, IEEE Microwaves and Wireless Components Letters. (2010). , 20(3), 176-177.

[24] Molina-cuberos, G. J, García-collado, A. J, Barba, I, & Margineda, J. Chiral Metamaterials with Negative Refractive Index Composed by an Eight-Cranks Molecule, IEEE Antennas and Wireless Propagation Letters. (2011). , 10-1488.

[25] García-collado, A. J, Molina-cuberos, G. J, & Núñez, M. J. Martín, Margineda J. Negative Refraction of Chiral Metamaterial Based on Four Crank Resonator, Journal of Electromagnetic Waves and Applications (2012). , 26-986.

[26] Agilent Technologies IncTime Domain Analysis Using a Network Analyzer, Application Note, (2012).

[27] Bohren, C. F. Light Scattering by an Optically Active Sphere. Chemical Physics Letters (1974). , 29-458.

[28] Varadan, V. V, & Ro, R. Unique Retrieval of Complex Permittivity and Permeability of Dispersive Materials from Reflection and Transmitted Fields By Enforcing Causality, IEEE Transactions on Microwave Theory and Techniques. (2007). , 55(10), 2224-2230.

[29] Chen, X, Grzegorczyk, T. M, Wu, B-I, Pacheco, J, & Kong, J. A. Robust Method to Retrieve the Constitutive Effective Parameters of Metamaterials. Physical Review E. (2004).

[30] Smith, D. R, Schultz, S, Markoš, P, & Soukoulis, C. M. Determination of Effective Permittivity and Permeability of Metamaterials from Reflection and Transmission Coefficients. Physical Review B. (2002).

[31] Ziolkowski, R. W. Design, Fabrication, and Testing of Double Negative Metamaterials. IEEE Transactions on Antennas and Propagation. (2003). , 7-1516.

[32] Condon, E. U. Theories of Optical Rotatory Power, Review Modern Physics. (1937). , 9-432.

[33] Hollinger, R, Varadan, V. V, & Varadan, V. K. Eigenmodes in a Circular Waveguide Containing an Isotropic Chiral Material, Radio Science. (1991). , 26(5), 1335-1344.

[34] Liu, Z, Sun, G, Huang, Q, & Yao, K. A Circular Waveguide Method for Measuring the Electromagnetic Parameters of Chiral Materials at Microwave Frequencies. Measurement Science Technolology. (1999). , 10-374.

[35] Reinert, J, Busse, G, & Jacob, A. F. Waveguide Characterization of Chiral Material: Theory. IEEE Trans. Microwave Theory and Techniques. (1999). , 47(3), 290-296.

[36] Lubkowski, G. Simulation of Electromagnetic Fields in Double Negative Metamaterials, Technishen Universität Darmstadt, PhD Dissertation, (2009).

[37] Barybin, A. A. Modal Expansions and Orthogonal Complements in the Theory of Complex Media Waveguide Excitation by External Sources for Isotropic, Anisotropic, and Bianisotropic Media, Progress in Electromagnetic Research, PIER (1998). , 19, 241-300.

[38] Tretyakov, S. A, & Viitanen, A. J. Perturbation Theory for a Cavity Resonator with a Biisotropic Sample: Application to Measurement Techniques, Microwave and Opt. Tech. Lett. (1992). , 5(4), 174-177.

[39] Tretyakov, S. A, & Viitanen, A. J. Waveguide and Resonator Perturbation Techniques Measuring Chirality and Nonreciprocity Parameters by Biisotropic Materials, IEEE Transactions on Microwave Theory and Techniques. (1995). , 43(1), 222-225.